Journal of Applied Fluid Mechanics, Vol. 10, No. 4, pp. 1105-1112, 2017.
Available online at www.jafmonline.net, ISSN 1735-3572, EISSN 1735-3645.
DOI: 10.18869/acadpub.jafm.73.241.27082

Effects of Thermal Radiation on MHD Peristaltic Motion of Walters-B Fluid with Heat Source and Slip Conditions

O. D. Makinde[1†], M. Gnaneswara Reddy[2] and K. Venugopal Reddy[2]

[1] *Faculty of Military Science, Stellenbosch University, Private Bag X2, Saldanha 7395,South Africa*
[2] *Department of Mathematics, Acharya Nagarjuna University Campus, Ongole-523 001, INDIA*

†*Corresponding Author Email: makinded@gmail.com*

(Received August 17, 2016; accepted February 25, 2017)

ABSTRACT

In this paper, we examine the combined effects of magnetic field, thermal radiation, heat source, velocity slip and thermal jump on peristaltic transport of an electrically conducting Walters-B fluid through a compliant walled channel. Using small wave number approach, the nonlinear model differential equations are obtained and tackled analytically by regular perturbation method. Expressions for the stream function, velocity, temperature, skin-friction coefficient and heat transfer coefficient are constructed. Pertinent results are presented graphically and discussed quantitatively. It is found that the velocity distribution depresses while the fluid temperature rises with an increase in Hartmann number. The trapping phenomenon is observed and the size of trapped bolus increases with an increase in Hartmann number.

Keywords: Thermal radiation; MHD; Peristalsis; Walter-B fluid; Compliant walls; Slip conditions; Heat generation.

1. INTRODUCTION

Peristalsis is a form of fluid shipment due to the induced wave traveling along the walls of the tube/channel. In physiology, peristalsis is used by the body to propel or mix the contents of a channel/tube. This mechanism take place in many biological systems such as transport of urine from kidney to bladder, food bolus through esophagus, transport of spermatozoa in vas deferens, food mixing and chymes transport in the intestine, transport of bile in the bile duct, transport of cilia and circulation of blood in small blood vessels. Some other significant applications are roller and finger pumps and blood pumps in heart lung machine. This phenomenon has also been exploited for industrial application like transport of corrosive fluids, transport of toxic liquid in nuclear industry and sanitary fluid transport. Academic interest and practical applications in physiology and industry have developed a lot of interest in studying the peristaltic flows in channels/tubes. Several experimental and theoretical studies have been undertaken after the pioneering work of Latham (1966). In particular, the theoretical investigations have been made under one or more simplified assumptions of long wavelength, low Reynolds number, small wave number, small amplitude ratio, etc. Extensive research on the topic has been carried out for the viscous and non-Newtonian fluids in a channel without compliant walls (Liron 1976; Makinde 1995; Makinde 2007). However, few recent attempts (Takabatake *et al.* 1988; Muthu *et al.* 2008) highlight the influence of wall properties on the peristaltic motion in a channel.

The peristaltic flows with heat transfer are important in the processes like hemodialysis and oxygenation. In view of such motivations, some researchers including Gnaneswara Reddy and Venugopal Reddy (2015) have conferred the influence of Joule heating on MHD peristaltic flow of a Nanofluid with compliant walls. The same authors (Gnaneswara Reddy and Venugopal Reddy 2016) have presented the impact of velocity slip and joule heating on MHD peristaltic flow through a porous medium with chemical reaction. Gnaneswara Reddy *et al*. (2016) have examined the hydromagnetic peristaltic motion of a reacting and radiating couple Stress fluid in an inclined asymmetric channel filled with a porous medium. Sarkar *et al*. (2015 studied the effects of magnetic field on peristaltic flow of nanofluids in a convectively heated vertical asymmetric channel in presence of thermal radiation.

Moreover, combined effects of thermal radiation and heat generation/absorption on hydromagnetic peristaltic flow is of considerable significance for

many scientific and engineering applications viz. heating and freezing of chambers, fossil fuel combustion energy processes, evaporation from massive open water reservoirs, propulsion devices for aircraft, missiles, satellites and space vehicles etc. Keeping in mind the importance of such applications investigated by several authors in (Adesanya and Makinde 2012; Seth *et al.* 2015a; Seth *et al.* 2015b; Seth *et al.* 2016)

Although in the peristaltic flow problems fewer attentions have been focused to analyze the flows in the presence of a slip condition. The application of slip condition in the peristaltic flows has special importance in physiology and polymers. It is now known that the no-slip conditions for velocity and the thermal conditions are not appropriate for momentum and heat transfer in micro devices. Walters-B fluid model with limiting viscosity at low shear rates and short memory coefficient (Beard and Walters 1964) is the best model for mentioned situations as discussed in literature Maryiam Javed *et al.* (2016) have analyzed the velocity and thermal slip effects on peristaltic motion of Walters-B fluid.

To the best of the author's knowledge no attempt has been done for thermal radiation and magnetohydrodynamic effects on the peristaltic flow of Walters-B fluid in a compliant wall. The purpose of the present investigation is to analyze the heat transfer and MHD effects on the peristaltic flow of Walters-B fluid in a compliant wall channel with thermal radiation and heat generation. The simplified equations are then solved using a regular perturbation method. Graphical results are presented for velocity, temperature, skin friction coefficient and heat transfer coefficient.

2. MODEL FORMULATION

Let us consider the unsteady peristaltic transport of an incompressible viscous electrically conducting and radiating of Walters-B fluid in a channel of width $2d$ (see Fig.1.). The channel walls are of compliant nature. The temperatures of the lower and upper walls of the channel are maintained at T_o and T_1 respectively. The geometry of the wall is

$$y = \pm\eta = \pm\left[d + a\sin\left(\frac{2\pi}{\lambda}(x - ct)\right)\right], \tag{1}$$

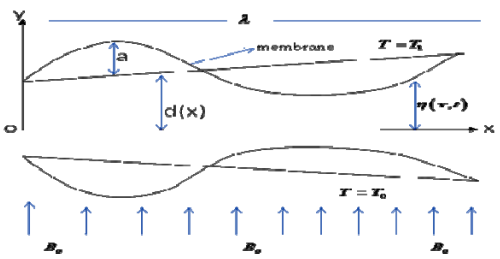

Fig.1. Geometry of the problem.

where λ is the wavelength, c is the wave speed, a is the wave amplitude and x and y are the Cartesian coordinates with x measured in the direction of the wave propagation and y measured in the direction normal to the mean position of the channel walls.

The flow problem for Walters-B fluid model is described as

The continuity equation:

$$\frac{\partial u}{\partial x} + \frac{\partial u}{\partial y} = 0, \tag{2}$$

The x component of momentum equation:

$$\rho\left(\frac{\partial}{\partial t} + u\frac{\partial}{\partial x} + v\frac{\partial}{\partial y}\right)u = -\frac{\partial p}{\partial x} + \frac{\partial S_{xx}}{\partial x} + \frac{\partial S_{xy}}{\partial y} - \sigma B_o^2 u, \tag{3}$$

The y component of momentum equation:

$$\rho\left(\frac{\partial}{\partial t} + u\frac{\partial}{\partial x} + v\frac{\partial}{\partial y}\right)v = -\frac{\partial p}{\partial y} + \frac{\partial S_{yx}}{\partial x} + \frac{\partial S_{yy}}{\partial y}, \tag{4}$$

where

$$S_{xx} = 4\eta_o\frac{\partial u}{\partial x} - 2\kappa_o\left[\begin{array}{l} 2\dfrac{\partial^2 u}{\partial x\partial t} + 2\left(u\dfrac{\partial^2 u}{\partial x^2} + v\dfrac{\partial^2 u}{\partial x\partial y}\right) - 4\left(\dfrac{\partial u}{\partial x}\right)^2 \\ -2\dfrac{\partial v}{\partial x}\left(\dfrac{\partial u}{\partial y} + \dfrac{\partial v}{\partial x}\right)\end{array}\right], \tag{5}$$

$$S_{xy} = 2\eta_o\left(\frac{\partial u}{\partial y} + \frac{\partial v}{\partial x}\right) - 2\kappa_o\left[\begin{array}{l} 2\dfrac{\partial^2 u}{\partial y\partial t} + \dfrac{\partial^2 v}{\partial x\partial t} - 2\dfrac{\partial u}{\partial x}\dfrac{\partial u}{\partial y} + \left(u\dfrac{\partial}{\partial x} + v\dfrac{\partial}{\partial y}\right)\left(\dfrac{\partial u}{\partial y} + \dfrac{\partial v}{\partial x}\right) \\ -\dfrac{\partial v}{\partial y}\left(\dfrac{\partial u}{\partial y} + \dfrac{\partial v}{\partial x}\right) - \left(\dfrac{\partial u}{\partial y} + \dfrac{\partial v}{\partial x}\right) - 2\dfrac{\partial v}{\partial x}\dfrac{\partial v}{\partial y}\end{array}\right], \tag{6}$$

$$S_{yy} = 4\eta_o\frac{\partial v}{\partial y} - 2\kappa_o\left[\begin{array}{l} 2\dfrac{\partial^2 v}{\partial y\partial t} + 2\left(u\dfrac{\partial^2 v}{\partial x\partial y} + v\dfrac{\partial^2 v}{\partial y^2}\right) - 4\left(\dfrac{\partial v}{\partial y}\right)^2 \\ -2\dfrac{\partial u}{\partial y}\left(\dfrac{\partial u}{\partial y} + \dfrac{\partial v}{\partial x}\right)\end{array}\right], \tag{7}$$

The energy balance equation is

$$\rho C_p\left(\frac{\partial}{\partial t} + u\frac{\partial}{\partial x} + v\frac{\partial}{\partial y}\right)T = \xi\nabla^2 T + \Phi - \frac{\partial q_r}{\partial y} + Q_o, \tag{8}$$

where

$$\Phi = S_{xx}\frac{\partial u}{\partial x} + S_{xy}\left(\frac{\partial u}{\partial y} + \frac{\partial v}{\partial x}\right) + S_{yy}\frac{\partial v}{\partial y}, \tag{9}$$

The equation governing the motion of flexible wall is expressed as

$$L(\eta) = p - p_o, \tag{10}$$

where p_o is pressure on the outside surface of the wall and L is an operator which represents the motion of stretched membrane with viscous damping forces such that

$$L = -\tau \frac{\partial^2}{\partial x^2} + m\frac{\partial^2}{\partial t^2} + d_1 \frac{\partial}{\partial t}, \tag{11}$$

in which τ is the elastic tension in the membrane, m is the mass per unit area and d_1 is the coefficient of damping. For simplicity we assume that p_o is zero. The continuity of stress at $y = \pm\eta(x,t)$ demands that the pressure exerted by the walls on the fluid is equal and opposite to the pressure exerted by the fluid on the walls. Further the deformation condition suggests that the transverse displacements of the walls are equal to the corresponding $y-$displacements of the fluid at the instantaneous positions of the interfaces. Combing the continuity of stress and condition of deformation the no-separation condition at the boundaries are

$$\frac{\partial}{\partial x}L(\eta) = \frac{\partial p}{\partial x} = \frac{\partial S_{xx}}{\partial x} + \frac{\partial S_{xy}}{\partial x} - \rho\left(\frac{\partial}{\partial t} + u\frac{\partial}{\partial x} + v\frac{\partial}{\partial y}\right)u,$$

at $y = \pm\eta(x,t)$. (12)

Such type of boundary condition is not restricted to the present problem. In fact it is also employed in other applications such as finishing of painted walls, frictional drag reduction on the hulls of ships and submarines etc. The radiative heat flux in the $X-$direction is considered as negligible compared to $Y-$direction. By using Rosseland approximation for thermal radiation, the radiative heat flux q_r is specified by

$$q_r = -\frac{16\sigma^* T_0^3}{3k^*}\frac{\partial T}{\partial y}, \tag{13}$$

where σ^* and k^* are the Stefan – Boltzmann constant and mean absorption coefficient respectively. The velocity and thermal slip conditions are

$$u \pm \beta_1 S_{xy} = 0$$

$$\text{at } y = \pm\eta(x,t) = \pm\left[d + a\sin\left(\frac{2\pi}{\lambda}(x - ct)\right)\right], \tag{14}$$

$$T \pm \beta_2 \frac{\partial T}{\partial y} = \begin{Bmatrix} T_1 \\ T_o \end{Bmatrix} \text{ at } \quad y = \pm\eta \tag{15}$$

Here u and v are the velocity components in the X and y directions respectively and ρ, t, p, η_o, K_o, ξ, T, Q_o and k^* are the fluid density, the time, the pressure, the limiting viscosity at small shear rates, the short memory coefficient, the specific heat, the thermal conductivity, the temperature , the dimensional heat absorption coefficient and the thermal conductivity respectively, β_1 is the velocity slip parameter and β_2 is the thermal slip parameter. Let

$$u = \frac{\partial \psi}{\partial y}, v = -\frac{\partial \psi}{\partial x}. \tag{16}$$

We introduce the following dimensionless parameters and variables;

$$x^* = \frac{x}{\lambda},\ y^* = \frac{y}{d},\ \psi^* = \frac{\psi}{cd},\ t^* = \frac{ct}{\lambda},\ \eta^* = \frac{\eta}{d},$$

$$\delta = \frac{d}{\lambda},\ \varepsilon = \frac{a}{d},\ p^* = \frac{d^2 p}{\eta_o c\lambda},\ \mathrm{Re} = \frac{cd}{\upsilon},\ \kappa = \frac{K_o c}{\eta_o d},$$

$$E_1 = -\frac{\tau d^3}{\lambda^3 \eta_o c}, E_2 = \frac{mcd^3}{\lambda^3 \eta_o}, E_3 = \frac{cd^3}{\lambda^2 \eta_o}, \beta_1^* = \frac{\beta_1}{d},$$

$$\beta_2^* = \frac{\beta_2}{d}\ \Phi^* = \frac{d^2}{\eta_o c^2}\Phi,\ \mathrm{Pr} = \frac{\eta_o C_p}{\xi}$$

$$E = \frac{c^2}{C_p(T_1 - T_o)},\ \theta = \frac{T - T_o}{T_1 - T_o}, M = \sqrt{\frac{\sigma}{\eta_o}}B_o d,$$

$$\beta = \frac{Q_o d^2}{\xi(T_1 - T_o)},\ Rd = \frac{16\sigma^* T_o^3}{3k^*\xi} \tag{17}$$

and dropping the asterisk for brevity, Eq. (2) is automatically satisfied and Eqs. (3) - (9) together with boundary conditions (14) and (15) with the help of (10) - (13), (16) and (17) take the form below:

$$\mathrm{Re}\delta\left(\psi_{yt} + \psi_y\psi_{xy} - \psi_x\psi_{yy}\right) = -\frac{\partial p}{\partial x} - M^2\frac{\partial \psi}{\partial y} + \delta S_{xx,x} + S_{xy,y} \tag{18}$$

$$\mathrm{Re}\delta^3\left(\psi_{xt} - \psi_y\psi_{xx} + \psi_x\psi_{xy}\right) = -\frac{\partial p}{\partial y} + \delta^2 S_{xy,x} + \delta S_{yy,y} \tag{19}$$

where

$$S_{xx} = 4\delta\psi_{xy} - 2\kappa\delta^2\begin{bmatrix} 2\psi_{xyt} + 2\left(\psi_y\psi_{xxy} - \psi_x\psi_{xyy}\right) \\ -4\psi_{xy}^2 + 2\psi_{xx}\left(\psi_{yy} - \delta^2\psi_{xx}\right) \end{bmatrix} \tag{20}$$

$$S_{xy} = 2\left(\psi_{yy} - \delta^2\psi_{xx}\right) - 2\kappa\begin{bmatrix} \delta\psi_{yyt} - \delta^3\psi_{xxt} + \delta\psi_y\psi_{xyy} - \delta^3\psi_y\psi_{xxx} \\ -\delta\psi_x\psi_{yyy} + \delta^3\psi_x\psi_{xxy} \\ -2\delta\psi_{xy}\psi_{yy} - 2\delta^3\psi_{xx}\psi_{xy} \end{bmatrix} \tag{21}$$

$$S_{yy} = -4\delta\psi_{xy} - 2\kappa\left[\delta^2\begin{pmatrix} -2\psi_{xyt} - 2\psi_y\psi_{xxy} + 2\psi_x\psi_{xyy} \\ +2\psi_{xx}\psi_{yy} - 4\psi_{yy}^2 \end{pmatrix} - 2\psi_{yy}^2\right], \tag{22}$$

$$\mathrm{PrRe}\delta\left(\frac{\partial\theta}{\partial t} + \psi_y\frac{\partial\theta}{\partial x} - \psi_x\frac{\partial\theta}{\partial y}\right) = \left(\frac{\partial^2\theta}{\partial y^2} + \delta^2\frac{\partial^2\theta}{\partial x^2}\right) + Br\Phi + \beta + Rd\frac{\partial^2\theta}{\partial y^2}, \tag{23}$$

$$\Phi = \delta S_{xx}\psi_{xy} + S_{xy}\left(\psi_{yy} - \delta^2\psi_{xx}\right) - \delta\psi_{xy}S_{yy}, \tag{24}$$

The associated boundary conditions are:

$$\psi_y \pm \beta_1 S_{xy} = 0,$$

$$\text{at} \quad y = \pm\eta = \pm\left[1 + \varepsilon\sin 2\pi(x - t)\right], \tag{25}$$

$$\frac{\partial p}{\partial x} = \left(\delta S_{xx,x} + S_{xy,y}\right) - \mathrm{Re}\,\delta\left[\psi_{yt} + \psi_y\psi_{xy} - \psi_x\psi_{yy}\right] - M^2\frac{\partial \psi}{\partial y}$$
$$= \left[E_1\frac{\partial^3}{\partial x^3} + E_2\frac{\partial^3}{\partial x\partial t^2} + E_3\frac{\partial^2}{\partial x\partial t}\right]\eta$$
at $y = \pm\eta$ (26)

$$\theta \pm \beta_2\theta_y = \begin{Bmatrix}1\\0\end{Bmatrix} \quad \text{at} \quad y = \pm\eta \tag{27}$$

where ψ is a stream function, M is the Hartmann number, Pr is the Prandtl number, Br($=Pr\,E$) is the Brinkman number, E is the Eckert number, δ is the wave number, Re is the Reynolds number, Rd is the Radiation parameter, β is the heat generation parameter, E_1, E_2 and E_3 are the non-dimensional compliant wall parameters.

3. PERTURBATION SOLUTION

In order to obtain the analytical solution of above mentioned problem, an effort has been made by employing power series expansion in the small parameter δ. This solution should be valid for any arbitrary set of values of all parameters used in mathematical model. Major equations governing the perturbation solution method are as follows:

$$\psi = \psi_0 + \delta\psi_1 + ..., \tag{28}$$

$$\theta = \theta_0 + \delta\theta_1 + ..., \tag{29}$$

$$S_{xx} = S_{xx0} + \delta S_{xx1} + ..., \tag{30}$$

$$S_{xy} = S_{xy0} + \delta S_{xy1} + ..., \tag{31}$$

$$S_{yy} = S_{yy0} + \delta S_{yy1} + ..., \tag{32}$$

$$Z = Z_0 + \delta Z_1 + ..., \tag{33}$$

The stream function is given by

$$\psi = C_2 y + C_4\sinh(Ny) + \delta\begin{pmatrix} C_6 y + C_8\sinh(Ny) + B_{21}y\cosh(Ny) \\ + B_{22}y^2\sinh(Ny) + B_{23}\sinh(Ny) \\ + B_{24}\sinh(2Ny)\end{pmatrix} \tag{34}$$

The velocity obtained from (16), which is given by

$$u = C_2 + C_4 N\cosh(Ny) + \delta\begin{pmatrix} C_6 + C_8 N\cosh(Ny) \\ + B_{21}\left(Ny\sinh(Ny) + \cosh(Ny)\right) \\ + B_{22}\left(Ny^2\cosh(Ny) + 2y\sinh(Ny)\right) \\ + B_{23}N\cosh(Ny) + 2B_{24}N\cosh(2Ny)\end{pmatrix} \tag{35}$$

The temperature is given by

$$\theta = D_1 + D_2 y + B_{43}\cosh(2Ny) + B_{44}y^2 + \delta\begin{pmatrix} D_3 + D_4 y + B_{138}y^2 + B_{139}y^3 + B_{140}y^4 + B_{141}\cosh(Ny) + B_{142}\sinh(Ny) \\ + B_{143}y\cosh(Ny) + B_{144}y\sinh(Ny) + B_{145}y\sinh(2Ny) + B_{146}\cosh(2Ny) \\ + B_{147}\cosh(3Ny) + B_{148}\cosh(4Ny) + B_{149}y\sinh(3Ny) + B_{150}y^2\cosh(2Ny) \\ + B_{151}y\cosh(3Ny) + B_{152}\sinh(3Ny) + B_{153}y^2\cosh(3Ny) + B_{154}y^2\cosh(Ny) \\ + B_{155}y\cosh(2Ny) + B_{156}\sinh(2Ny) + B_{157}y^3\sinh(2Ny) \\ + B_{158}y^4\cosh(2Ny) + B_{159}y^6\end{pmatrix} \tag{36}$$

The shear stress and heat transfer rate at the wall are defined in terms of skin friction coefficient (C_f) and Nusselt number (Nu) as follows:

$$C_f = \eta_x\left(\psi_{0yy} + \delta\psi_{1yy}\right), \tag{37}$$

$$Z = \eta_x\left(\theta_{0y} + \delta\theta_{1y}\right), \tag{38}$$

where the constants are involved in Eqs. (34) – (36) can obtained through simple algebraic computations.

4. RESULTS AND DISCUSSION

In this section, the numerical results of the analytical expressions obtained for the fluid velocity, temperature, skin friction and Nusselt number are displayed graphically in Figs. 2 - 16 and discussed quantitatively. The following parameter values are utilized for numerical computations: E_1=1, E_2=0.4, E_3=0.5, Re=1, x=0.5, t=0.8, M=3, Br=0.8, Rd=1, Pr=0.7, β_1=0.1, β_2=0.01, β=0.1, ε=0.01, κ=2, δ=0.01.

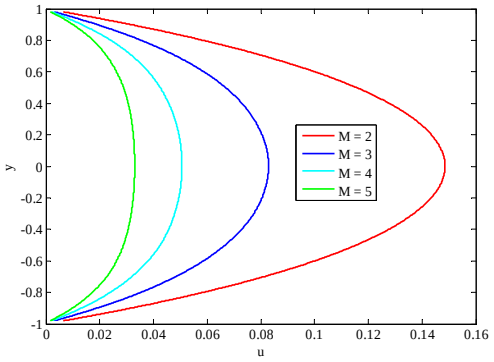

Fig. 2. Effect of M on velocity profile.

4.1 Velocity Distribution

Figs. 2 – 4 show the behavior of parameters involved in the velocity u. Fig.2. depicts that the velocity reduces as M increases because of the Lorentz force associated with the applied magnetic field along the transverse direction which opposes the flow. Fig.3. reveals that the velocity depresses with increase of β_1 due to wall slip. Fig.4. shows the behavior of compliant wall parameters E_1, E_2 and E_3 on the fluid velocity. It is found that the velocity

diminishes with an increase in wall damping coefficient E_3. This parameter has oscillatory resistance to the flow that's why velocity decreases with wall damping coefficient E_3. The velocity is increasing function of E_1 and E_2 physically means that the wall elastance assists the flow. Also the velocity profile is parabolic for fixed values of the parameter and its magnitude is maximum near the center of the channel.

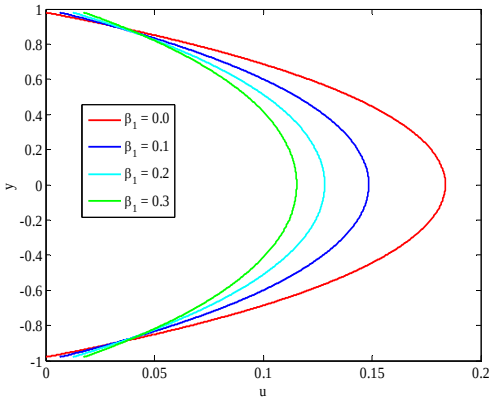

Fig. 3. Effect of β_1 on velocity profile.

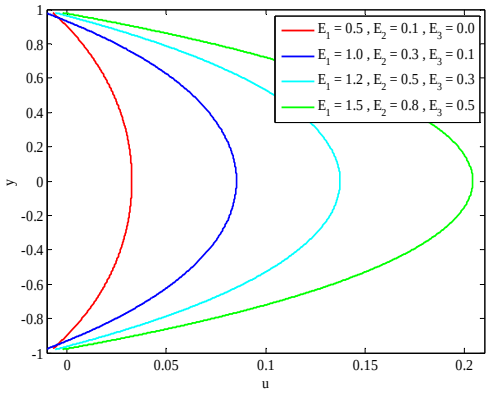

Fig. 4. Effect of E_1, E_2 and E_3 on velocity profile.

4.2 Temperature Distribution

The effect of various physical parameters on the temperature is shown in Figs. 5 – 8. The nature of temperature is parabolic through all figures. In Figs. 5 and 6 we observed that the fluid temperature rises with an increase in Hartmann number M and the thermal slip parameter β_2. It may also be noted from Fig. 6 that for any values of β_2, temperature increases with the height of the channel after attaining its maximum, it decreases. An increase in thermal radiation Rd absorption decreases the fluid temperature as shown in Fig.7. Fig.8. emphasizes that as heat generates during blood flow in arterioles, there is a significant increase in thickness of boundary layer as heat generation parameter β enhances. Thereby the temperature of the boundary layer increased by appreciable extend.

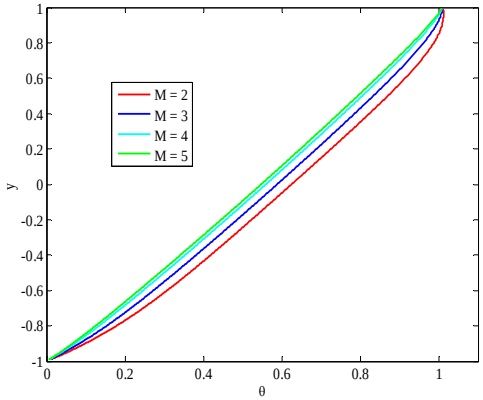

Fig. 5. Effect of M on temperature profile.

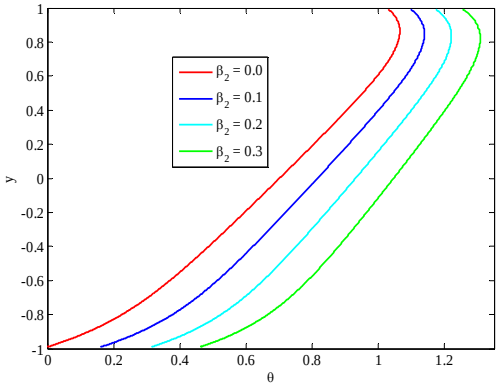

Fig. 6. Effect of β_2 on temperature profile.

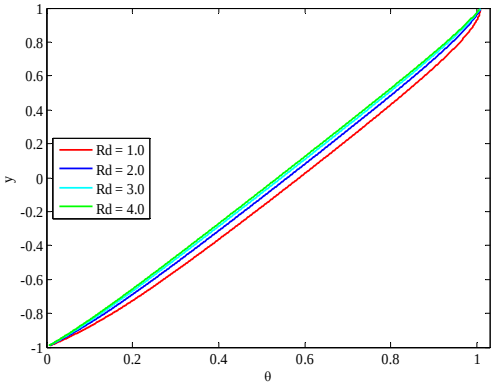

Fig. 7. Effect of Rd on temperature profile.

4.3 Skin-Friction Coefficient

The effect of various physical parameters on the skin-friction coefficient is shown in Figs. 9 – 10. The absolute value of skin – friction coefficient enhances with an increase in Hartmann number M and velocity slip parameter β_1.

4.4 Heat Transfer Coefficient

Figs. 11 – 13 depict the effects of thermophysical parameters on heat transfer coefficient. Heat transfer coefficient has oscillatory behavior which is expected in view of peristalsis and complaint wall

effects. Fig.11 shows that the heat transfer coefficient enhances when M increases. Fig. 12 and 13 show that the heat transfer coefficient depresses when an increase in Rd and β .

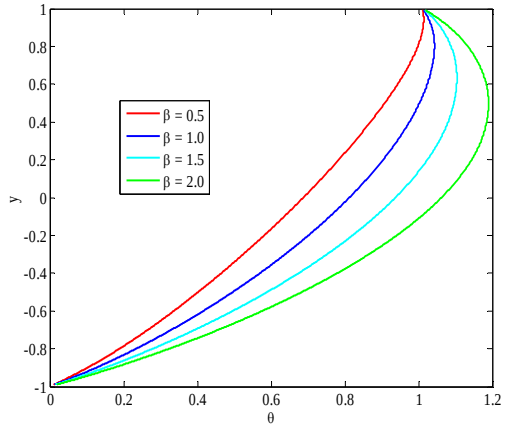

Fig. 8. Effect of β on temperature profile.

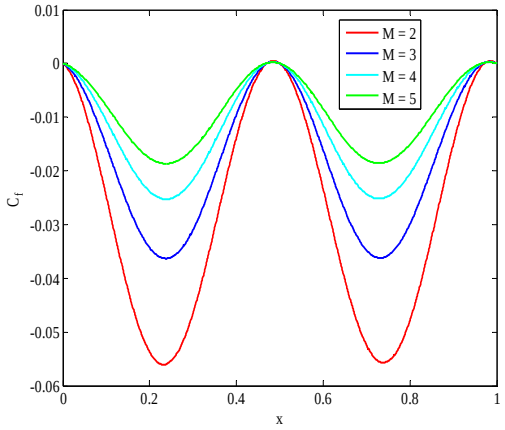

Fig. 9. Effect of M on skin-friction coefficient.

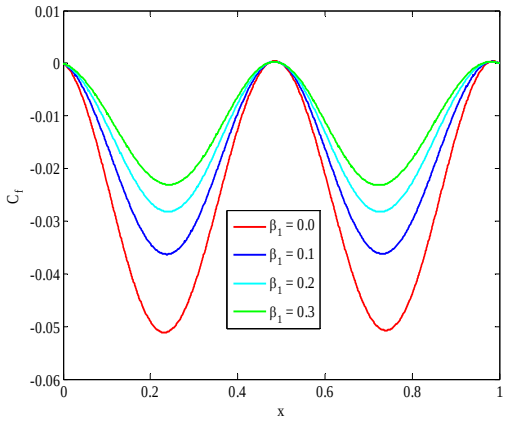

Fig. 10. Effect of β_1 on skin-friction coefficient.

4.5 Trapping Phenomenon

Trapping is an important phenomenon in peristaltic motion. Generally the shape of streamlines shows the effect of boundary wall on the flow pattern. Interestingly, the streamlines split to form re-circulating closed streamlines called bolus within the channel. Figs. 14 and 15 revealed that that the size of trapped bolus increases with a rise in the intensity of magnetic field M.

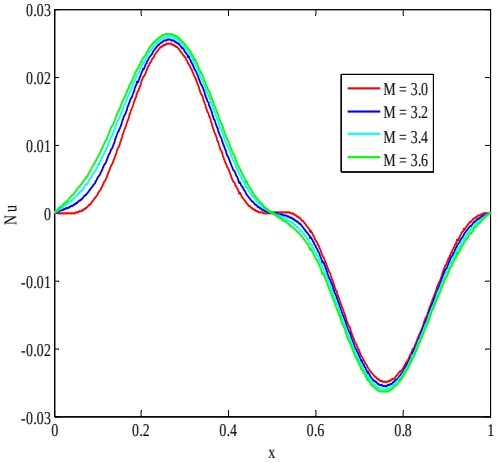

Fig. 11. Effect of M on Nusselt number.

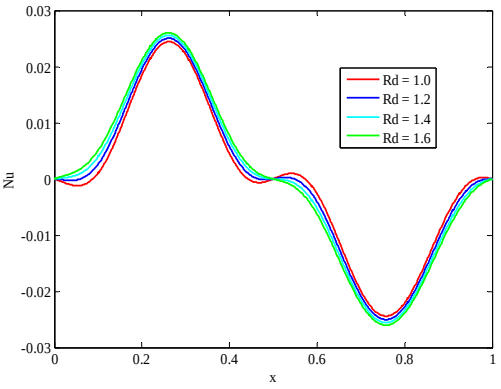

Fig. 12. Effect of Rd on Nusselt number.

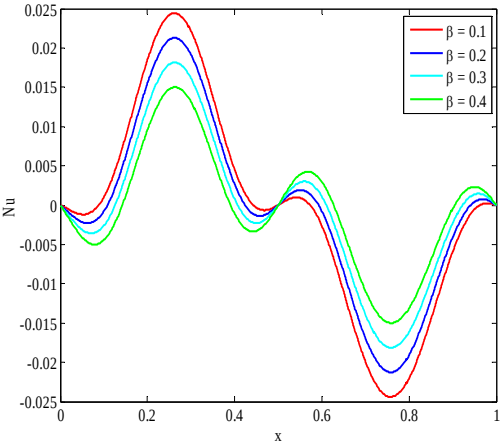

Fig. 13. Effect of β on Nusselt number.

Validation: Comparison of a special case of our present study (i.e. Rd=0, M=0, β=0) with that of recent results presented by Javed *et al.* (2016) is presented in Fig.16 and an excellent agreement is observed.

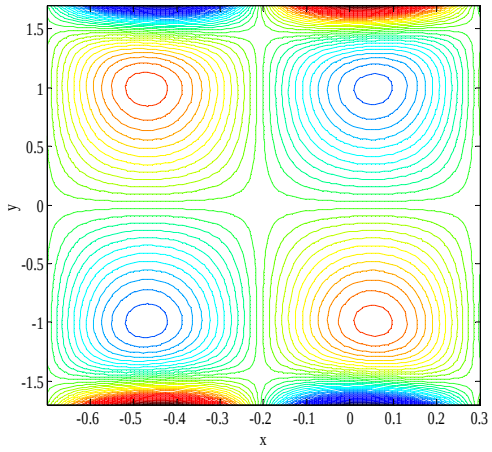

Fig. 14. Stream lines for $M = 3$.

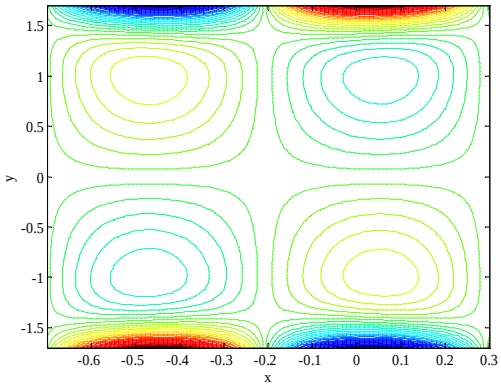

Fig. 15. Stream lines for $M = 4$.

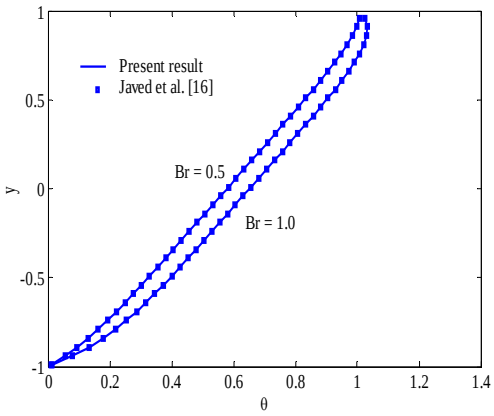

Fig. 16. Comparison results with Javed *et al.* (2016).

5. CONCLUDING REMARKS

This study examines the influence of thermal radiation absorption on the peristaltic flow of hydromagnetic Walter-B fluid flow with heat transfer through a compliant walled channel. The analytical solution has been evaluated using regular perturbation method. The expressions for velocity, temperature, skin-friction coefficient, heat transfer coefficient and stream function have been discussed graphically. The following observations have been found:

- The velocity field diminishes with an increase in M and β_1.
- The fluid temperature rises with an increase M and β but decreases with Rd.
- The absolute value of skin friction coefficient increases with an increase in M.
- The heat transfer coefficient increases with an increase M and Rd, while the opposite trend is observed with an increase in β.
- Size of trapped bolus increases with an increase in Hartmann number M.

REFERENCES

Adesanya, S. O. and O. D. Makinde (2012). Heat transfer to magnetohydrodynamic non-Newtonian couple stress pulsatile flow between two parallel porous plates. *Zeitschrift f¨ur Naturforschung* 67a, 647 – 656.

Beard, D. W. and K. Walters (1964). Elastico-viscous boundary-layer flows. Part I. Two-dimensional flow near a stagnation point. *Proc. Camb. Phil. Soc.*, 60, 667-674.

Gnaneswara Reddy, M. and K. Venugopal Reddy (2015). Influence of Joule heating on MHD peristaltic flow of a Nanofluid with compliant walls. *Procedia Engineering*, 127, 1002–1009.

Gnaneswara Reddy, M. and K. Venugopal Reddy (2016). Impact of velocity slip and Joule heating on MHD peristaltic flow through a porous medium with chemical reaction. *Journal of the Nigerian Mathematical Society* 35, 227-244.

Gnaneswara Reddy, M., K. Venugopal Reddy and O. D. Makinde (2016). Hydromagnetic peristaltic motion of a reacting and radiating couple Stress fluid in an inclined asymmetric channel filled with a porous medium**.** *Alexandria Engineering Journal* 55, 1841–1853.

Javed, M., T. Hayat, M. Mustafa and B. Ahmad (2016). Velocity and thermal slip effects on peristaltic motion of Walters-B fluid. *International Journal of Heat and Mass Transfer* 96, 210–217.

Latham, T. W. (1966). *Fluid motion in a peristaltic pump*. MIT Press, Cambridge Mass, USA.

Liron, N. (1976). On peristaltic flow and its efficiency. *Bull. Math. Biol.* 38, 573–596.

Makinde, O. D. (1995). Laminar flow in a channel of varying width with permeable boundaries. *Romanian Jour. Phys. 40(4/5), 403-417.*

Makinde, O. D. (2007). Asymptotic approximations for oscillatory flow in a tube of varying cross-section with permeable isothermal wall. *Romanian Journal of Physics 52(1/2), 59-72.*

Muthu, P., B. V. R. Kumar and P. Chandra (2008).

Peristaltic motion of micropolar fluid in circular cylindrical tubes: effect of wall properties. *Appl. Math. Model*. 32, 2019–2033.

Sarkar, B. C., S. Das, R. N. Jana and O. D. Makinde (2015). Magnetohydrodynamic peristaltic flow of nanofluids in a convectively heated vertical asymmetric channel in presence of thermal radiation. *Journal of Nanofluids* 4(4), 461-473.

Seth, G. S., B. Kumbhakar and R. Sharma (2015b). Unsteady hydromagnetic natural convection flow of a heat absorbing fluid within a rotating vertical channel in porous medium with Hall effects. *Journal of Applied Fluid Mechanics* 8(4), 767-779.

Seth, G. S., R. Sharma and B. Kumbhakar (2106). Heat and mass transfer effects on unsteady MHD natural convection flow of a chemically reactive and radiating fluid through a porous medium past a moving vertical plate with arbitrary ramped temperature. *Journal of Applied Fluid Mechanics* 9(1), 103-117.

Seth, G. S., R. Sharma and S. Sarkar (2015a). Natural convection heat and mass transfer flow with Hall current, rotation, radiation and heat absorption past an accelerated moving vertical plate with ramped temperature. *Journal of Applied Fluid Mechanics* 8(1). 7-20.

Takabatake, S., K. Ayukawa and A. Mori (1988). Peristaltic pumping in circular cylindrical tubes: a numerical study of fluid transport and its efficiency, *J. Fluid Mech.* 193, 267–283.